A simple model predicts how warming simplifies wild food webs

Eoin J. O'Gorman[1,*], Owen L. Petchey[2], Katy J. Faulkner[3], Bruno Gallo[4],

Timothy A.C. Gordon[5], Joana Neto-Cerejeira[2], Jón S. Ólafsson[6], Doris E.

Pichler[4], Murray S.A. Thompson[7], and Guy Woodward[4,*].

[1] *School of Biological Sciences, University of Essex, Wivenhoe Park, Colchester, CO4 3SQ, UK.*

[2] *Institute of Evolutionary Biology and Environmental Studies, University of Zurich,*

Winterthurerstrasse 190, CH-8057 Zurich, Switzerland.

[3] *School of Life Sciences, Gibbet Hill Campus, University of Warwick, Coventry, CV4 7AL, UK.*

[4] *Department of Life Sciences, Imperial College London, Silwood Park Campus, Buckhurst Road,*

Ascot, Berkshire, SL5 7PY, UK.

[5] *Biosciences, College of Life and Environmental Sciences, University of Exeter, Stocker Road,*

Exeter, EX4 4QD, UK.

[6] *Marine and Freshwater Research Institute, Skúlagata 4, 101 Reykjavík, Iceland.*

[7] *Centre for Environment, Fisheries & Aquaculture Science, Pakefield Road, Lowestoft, Suffolk, NR33*

0HT, UK.

Running head: Warming simplifies food webs

Type of paper: Letter

* Corresponding authors: Eoin O'Gorman; Guy Woodward

E-mail: e.ogorman@essex.ac.uk; guy.woodward@imperial.ac.uk

Tel: +44 1206 876389; +44 20 7594 2237

1

Warming increases the metabolic demand of consumers[1], strengthening their feeding interactions[2]. This could alter energy fluxes[3-5] and even amplify extinction rates within the food web[6-8]. Such effects could simplify the structure and dynamics of ecological networks[9,10], although an empirical test in natural systems has been lacking. Here, we tested this hypothesis by characterising ~50,000 directly observed feeding interactions across 14 naturally heated stream ecosystems[11-15]. We found that higher temperature simplified food web structure and shortened the pathways of energy flux between consumers and resources. A surprisingly simple allometric diet breadth model[10,16] predicted 68-82% of feeding interactions and the effects of warming on key food web properties. We used model simulations to identify the underlying mechanism as a change in the relative diversity and abundance of consumers and their resources. This shows how warming can reduce the stability of aquatic ecosystems by eroding the structural integrity of the food web. Given these fundamental drivers, such responses are expected to be manifested more broadly and could be predicted using our modelling framework and knowledge of how warming alters some routinely measured characteristics of organisms.

All natural systems contain complex food webs, whose stability is shaped by non-random structural properties[17], *e.g.* the strength of consumer-resource interactions[18,19] and the flow of energy from many abundant small species into progressively fewer large species, especially in the aquatic realm[20]. Global warming could disrupt these patterns, yet we lack high quality field data to test and validate predictive models of temperature effects on food webs. In theory, consumers should exert stronger feeding pressure on the biomass stocks of lower trophic levels in warmer environments[3,4], but may struggle to meet their rising energy demands[7,8]. This could lead to shorter food chains[6], simpler food webs[9], less efficient energy flux[5], and an altered distribution of biomass through the food web[21].

26 To test these expectations, we exhaustively characterised food web interactions for 14

27 geothermally heated streams in Iceland using dietary analysis (see Methods). The streams

28 occur within 1.5 km of each other in a pristine mountain landscape (Fig. S1), free from

29 anthropogenic influences apart from occasional sheep grazing. The streams are very similar

30 in their physical and chemical properties and yet vary in temperature from 5-25 °C due to

31 indirect heating of groundwater through the bedrock (Tables S1-S3). Since the streams occur

32 in the same catchment, they avoid the biogeographical differences associated with other

33 natural gradients in temperature (*e.g.* latitude or altitude)[22]. This study system thus acts as a

34 space-for-time proxy, where temperature effects on food web structure can be investigated in

35 a wild setting with all the complexity and realism of natural ecosystems[22].

36 We used an allometric diet breadth model (ADBM)[10,16], parameterised with data on the

37 average body mass and population abundance of species sampled in each stream in August

38 2008 (*i.e.* no *a priori* information on feeding links), to predict the structure of each food web

39 (see Methods). We then examined how several properties of the ADBM-predicted food webs

40 varied with stream temperature, finding significant linear relationships for four key metrics

41 related to food chain length, complexity, energy flux, and biomass distribution (Fig. S2). This

42 allowed us to formulate four hypotheses (H1-4) that could be tested with an empirical

43 quantification of feeding links in the system. We anticipate that, as stream temperature

44 increases, there will be: (H1) a reduction in mean trophic level; (H2) a decrease in

45 connectance; (H3) shorter pathways of energy flux through the food web; and (H4) an

46 increasing biomass of consumers relative to their resources.

47 We tested our predictions by characterising the actual food web structure of each

48 stream based on almost 50,000 gut content observations (see Methods). There was a

49 simplification of food web structure as stream temperature increased, from a diffuse,

50 reticulate network (Fig. 1a) to one with fewer and shorter chains (Fig. 1b). In support of H1,

mean trophic level was lower in the warmer streams (Fig. 1c), with herbivorous interactions becoming increasingly dominant. This appeared to be driven by a disproportionate loss of consumer species, relative to resources, as stream temperature increased (Fig. S3). Consumer losses likely occurred as they were unable to meet the greater metabolic demands of the warmer environment[1,7] and/or withstand increased predation by an apex predator, brown trout, which cannot persist in the coldest streams due to its own metabolic constraints[13,14]. Warmer food webs were also less connected (Fig. 1d), as expected in H2, suggesting they will be more sensitive to secondary extinctions[23,24] and dominated by more specialised consumers, with energy channelled through fewer and stronger links[9]. Similar patterns were obtained when the same streams were sampled again in April 2009 (Fig. S4a,b).

To assess how these structural changes altered energy flux through the food web, we calculated the lengths and angles of all pairwise consumer-resource links in $\log_{10}$(body mass) and $\log_{10}$(abundance) space[25] (see Fig. 2a,b for definitions of these terms). The average pathway of energy flux through the food web was shorter in warmer streams (Fig. 2c,d), due to a reduction in mean link length as temperature increased (Fig. 2e). This supports H3 and points to stronger feeding pressure in the warmer streams[13,14], with the abundance of resources suppressed relative to their consumers (Fig. S5b). A link angle of -45° means that resource biomass equals consumer biomass[25] (Fig. 2a) and mean link angle became progressively smaller than this at higher temperatures (Fig. 2f). This indicates that the biomass of consumers was on average greater than the biomass of their resources in the warmer streams (Fig. S5c, S6), as predicted in H4. Inverted biomass pyramids are promoted by stronger top-down control, generalist feeding, larger predators, and higher trophic transfer efficiency[21,26], all of which have been documented to increase with stream temperature in the Hengill system[12-14]. They can only persist, however, if resources are replenished rapidly enough to meet the metabolic demands of consumers[12], *i.e.* the standing stock of resources is

76 low, but production is high enough to maintain consumer biomass through time. Such top-

77 heaviness is increasingly documented in nature when consumer pressure or anthropogenic

78 disturbance is especially powerful (*e.g.* in marine fisheries), but these systems are less stable

79 than their pyramidal counterparts[21,27]. We found similar patterns for mean link angle, but no

80 effect on mean link length from the April 2009 sampling (Fig. S4c,d), suggesting that effects

81 of temperature on the latter in August 2008 should be treated with caution.

82   Our model accurately predicted a higher proportion of empirically observed feeding

83 interactions than previously documented for high quality food webs[16]: 75 ± 3.9 % (mean ±

84 standard deviation) across all 14 streams (Fig. S7). This shows that the ADBM can be a

85 useful tool for predicting ecological networks[16], at least for size-structured aquatic

86 ecosystems like our study streams[12], even when interaction data are limited, as is the case for

87 most studies to date[28]. Our empirical measures of food web structure and energy flux were

88 also strongly correlated with the ADBM predictions, although deviation of the slope from the

89 1:1 line suggests the model did not produce an accurate quantitative prediction of

90 connectance (Fig. S8). Our results indicate that the ADBM can also predict the impacts of

91 temperature on natural food webs, using simple information that is routinely collected in

92 ecological field studies. Further testing of the model with other highly resolved food web

93 datasets from experiments that have manipulated warming in a controlled fashion would

94 validate this suggestion more broadly.

95   As a final exploratory step, we investigated the underpinning mechanisms by using the

96 ADBM to simulate food webs after changing one of the three major input variables: species

97 identity, average body mass, and population abundance. By randomly choosing species from

98 the regional species pool ('*sp*' scenario), we disrupted the trophic structure of any given

99 stream and thus the relationship between stream temperature and the ratio of consumer to

100 resource species richness (Fig. 3a). By randomly choosing a mean body mass ('*M*' scenario)

101   or population abundance ('*N*' scenario) for each species from the same trophic groups in the

102   regional dataset, we disrupted the relationship between stream temperature and the ratio of

103   consumer to resource body mass or abundance, respectively (Fig. 3b,c). For each scenario,

104   we then simulated 1,000 food webs for each of our 14 study streams after randomising one

105   input variable and fixing the values of the other two variables as close to the real stream as

106   possible (see Methods).

107   Our '*sp*' scenario removed the effect of temperature on mean trophic level and

108   connectance (Fig. 3d,e), with negligible effects of the other two scenarios. This suggests that

109   the relative biodiversity of consumers and resources is a key determinant of these food web

110   properties. We used the 14,000 food webs simulated under the '*sp*' scenario to explore this

111   effect, independent of temperature, and found that both mean trophic level and connectance

112   increase with the ratio of consumer to resource species richness (Fig. 4a,b). Thus, the

113   disproportionate loss of consumer species, which is widely predicted in response to

114   warming[6-8], should lead to reductions in these food web properties.

115   While all three randomisation scenarios disrupted temperature effects on link lengths

116   and angles, our '*N*' scenario had by far the greatest effect (Fig. 3f,g), suggesting the ratio of

117   consumer to resource abundance is the principal determinant of energy flux. We used the

118   food webs simulated under the '*N*' scenario to explore this effect, independent of temperature,

119   and found that link lengths and angles become smaller as consumers approach the abundance

120   of their resources (Fig. 4c,d). Thus, stronger top-down control that alters the shape of trophic

121   abundance pyramids, which is often reported in warmer environments[3,4], will suppress energy

122   flux through the food web.

123   Our study is one of the first to show systematic impacts of temperature on wild food

124   webs (*e.g.* see also[29]). Most riverine ecosystems in Europe and North America fall within the

125   studied temperature gradient of 5-25 °C[30] and so our results should be indicative of changes

126 in food web structure due to future warming within this range. Our findings highlight the
127 importance of monitoring species interactions for successful management of ecosystems[31],
128 given that trophic structure is so sensitive to environmental change. For example, mean
129 trophic level is increasingly used in fisheries management to identify overfishing at the top of
130 the food web[32], while connectance is a useful indicator of resistance to invasion[33] and
131 robustness against biodiversity loss[23,24]. We identified changes in the relative biodiversity or
132 abundance of consumers and resources at higher temperatures as key mechanisms driving the
133 observed effects. Such changes are also elicited by anthropogenic activities like
134 overexploitation and habitat degradation[32,34], emphasising how the structure and stability of
135 ecological networks may be threatened by a host of stressors. The predictive power of our
136 model shows how the impact of these stressors could be anticipated and ultimately mitigated
137 more broadly. These findings now need to be tested in a range of food webs from marine,
138 freshwater, and terrestrial realms to gauge their potential universality.

149 **Author contributions**

150   EJOG, OLP, and GW were responsible for funding application, research design, and

151 planning. EJOG, KJF, BG, TACG, JNC, JSÓ, DEP, and MSAT collected the data. EOG and

152 OLP analysed the data. All authors wrote the paper.

153 **References**

154   1   Brown, J. H., Gillooly, J. F., Allen, A. P., Savage, V. M. & West, G. B. Toward a

155   metabolic theory of ecology. *Ecology* **85**, 1771-1789 (2004).

156   2   Rall, B. C. *et al.* Universal temperature and body-mass scaling of feeding rates.

157   *Philosophical Transactions of the Royal Society B: Biological Sciences* **367**, 2923-

158   2934 (2012).

159   3   O'Connor, M. I., Piehler, M. F., Leech, D. M., Anton, A. & Bruno, J. F. Warming and

160   resource availability shift food web structure and metabolism. *PLoS Biology* **7**,

161   e1000178 (2009).

162   4   Shurin, J. B., Clasen, J. L., Greig, H. S., Kratina, P. & Thompson, P. L. Warming

163   shifts top-down and bottom-up control of pond food web structure and function.

164   *Philosophical Transactions of the Royal Society B: Biological Sciences* **367**, 3008-

165   3017 (2012).

166   5   Schwarz, B. *et al.* Warming alters energetic structure and function but not resilience

167   of soil food webs. *Nature Climate Change* **7**, 895-900 (2017).

168   6   Petchey, O. L., McPhearson, P. T., Casey, T. M. & Morin, P. J. Environmental

169   warming alters food-web structure and ecosystem function. *Nature* **402**, 69-72 (1999).

170   7   Vucic-Pestic, O., Ehnes, R. B., Rall, B. C. & Brose, U. Warming up the system:

171   higher predator feeding rates but lower energetic efficiencies. *Global Change Biology*

172   **17**, 1301-1310 (2011).

8   Fussmann, K. E., Schwarzmüller, F., Brose, U., Jousset, A. & Rall, B. C. Ecological stability in response to warming. *Nature Climate Change* **4**, 206-210 (2014).

9   Binzer, A., Guill, C., Rall, B. C. & Brose, U. Interactive effects of warming, eutrophication and size-structure: impacts on biodiversity and food-web structure. *Global Change Biology* **22**, 220-227 (2016).

10   Petchey, O. L., Brose, U. & Rall, B. C. Predicting the effects of temperature on food web connectance. *Philosophical Transactions of the Royal Society B: Biological Sciences* **365**, 2081-2091 (2010).

11   Friberg, N. *et al.* Relationships between structure and function in streams contrasting in temperature. *Freshwater Biology* **54**, 2051-2068 (2009).

12   O'Gorman, E. J. *et al.* Unexpected changes in community size structure in a natural warming experiment. *Nature Climate Change* **7**, 659-666 (2017).

13   O'Gorman, E. J. *et al.* Impacts of warming on the structure and functioning of aquatic communities: individual- to ecosystem-level responses. *Advances in Ecological Research* **47**, 81-176 (2012).

14   O'Gorman, E. J. *et al.* Temperature effects on fish production across a natural thermal gradient. *Global Change Biology* **22**, 3206-3220 (2016).

15   Adams, G. *et al.* Diatoms can be an important exception to temperature-size rules at species and community levels of organization. *Global Change Biology* **19**, 3540-3552 (2013).

16   Petchey, O. L., Beckerman, A. P., Riede, J. O. & Warren, P. H. Size, foraging, and food web structure. *Proceedings of the National Academy of Sciences of the United States of America* **105**, 4191-4196 (2008).

17   Pimm, S. L. *Food Webs*. (University of Chicago Press, 1982).

18   Allesina, S. & Tang, S. Stability criteria for complex ecosystems. *Nature* **483**, 205-

198 208 (2012).

199 19 McCann, K., Hastings, A. & Huxel, G. R. Weak trophic interactions and the balance

200   of nature. *Nature* **395**, 794-798 (1998).

201 20 Elton, C. S. *Animal Ecology*. (Sidgwick & Jackson, 1927).

202 21 McCauley, D. J. *et al.* On the prevalence and dynamics of inverted trophic pyramids

203   and otherwise top-heavy communities. *Ecology Letters* **21**, 439-454 (2018).

204 22 O'Gorman, E. J. *et al.* Climate change and geothermal ecosystems: natural

205   laboratories, sentinel systems, and future refugia. *Global Change Biology* **20**, 3291-

206   3299 (2014).

207 23 Dunne, J. A., Williams, R. J. & Martinez, N. D. Network structure and biodiversity

208   loss in food webs: robustness increases with connectance. *Ecology Letters* **5**, 558-567

209   (2002).

210 24 Gilbert, A. J. Connectance indicates the robustness of food webs when subjected to

211   species loss. *Ecological Indicators* **9**, 72-80 (2009).

212 25 Cohen, J. E., Schittler, D. N., Raffaelli, D. G. & Reuman, D. C. Food webs are more

213   than the sum of their tritrophic parts. *Proceedings of the National Academy of*

214   *Sciences* **106**, 22335-22340 (2009).

215 26 Woodson, C. B., Schramski, J. R. & Joye, S. B. A unifying theory for top-heavy

216   ecosystem structure in the ocean. *Nature communications* **9**, 23 (2018).

217 27 Neutel, A. M., Heesterbeek, J. A. P. & de Ruiter, P. C. Stability in real food webs:

218   Weak links in long loops. *Science* **296**, 1120-1123 (2002).

219 28 Ings, T. C. *et al.* Ecological networks - beyond food webs. *Journal of Animal Ecology*

220   **78**, 253-269 (2009).

221 29 Tunney, T. D., McCann, K. S., Lester, N. P. & Shuter, B. J. Effects of differential

222   habitat warming on complex communities. *Proceedings of the National Academy of*

223   *Sciences* **111**, 8077-8082 (2014).

224 30 Van Vliet, M., Ludwig, F., Zwolsman, J., Weedon, G. & Kabat, P. Global river

225   temperatures and sensitivity to atmospheric warming and changes in river flow. *Water*

226   *Resources Research* **47** (2011).

227 31 Gray, C. *et al.* Ecological networks: the missing links in biomonitoring science.

228   *Journal of Applied Ecology* **51**, 1444-1449 (2014).

229 32 Branch, T. A. *et al.* The trophic fingerprint of marine fisheries. *Nature* **468**, 431-435

230   (2010).

231 33 Smith-Ramesh, L. M., Moore, A. C. & Schmitz, O. J. Global synthesis suggests that

232   food web connectance correlates to invasion resistance. *Global Change Biology* **23**,

233   465-473 (2017).

234 34 Barnes, A. D. *et al.* Consequences of tropical land use for multitrophic biodiversity

235   and ecosystem functioning. *Nature Communications* **5**, 5351 (2014).
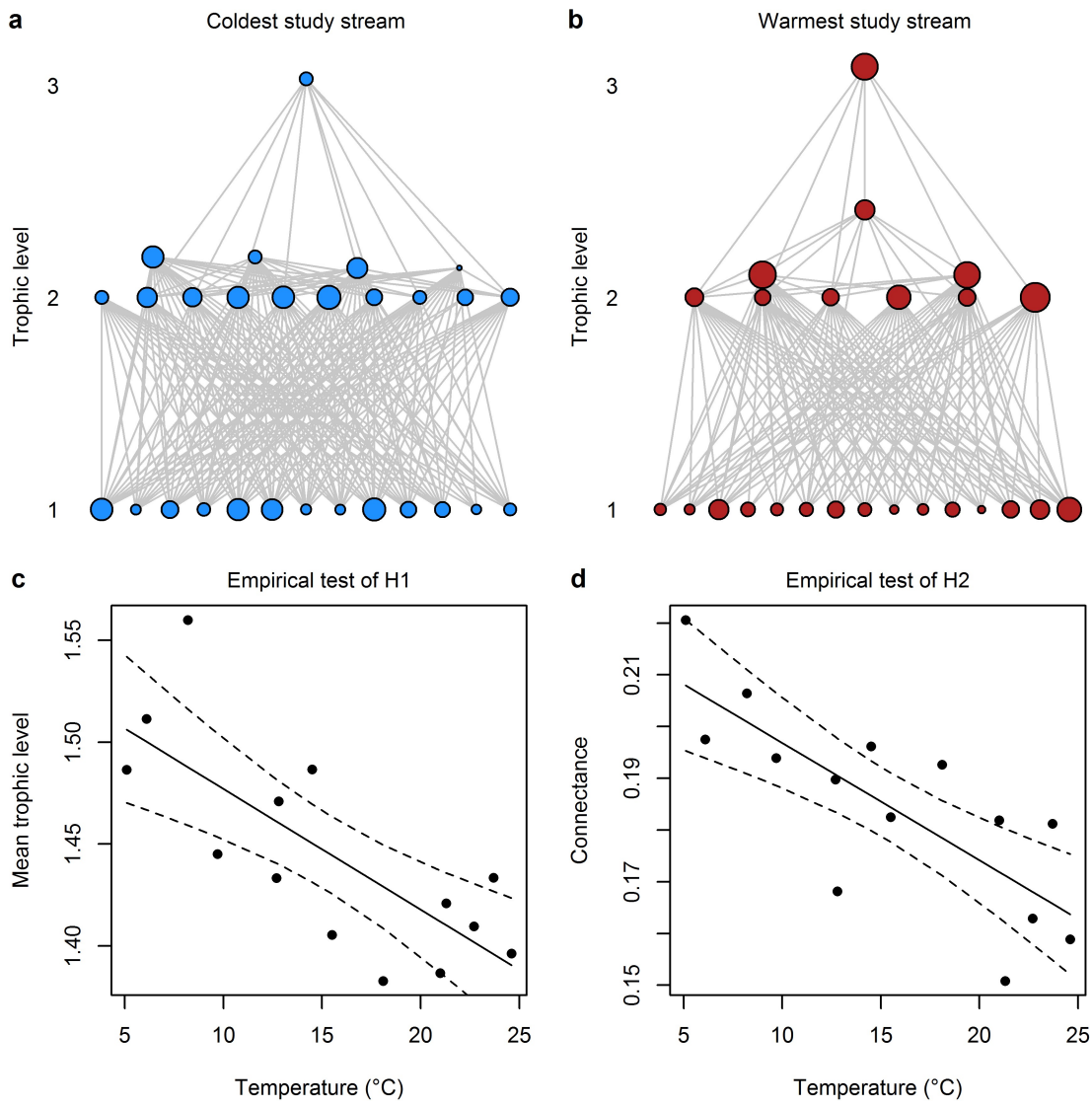
236

Figure Legends

238 **Fig. 1. Temperature effects on food web properties.** Food webs for the (**a**) coldest and (**b**)

239 warmest stream in the system, where circles are species, grey lines are feeding interactions,

240 and the size of the circles is proportional to the population biomass of each species in the

241 stream. Note the reduction in the number of consumer species in the food web for the warm

242 stream and the 'thinning out' of feeding interactions compared to the cold stream. There was a

243 reduction in (**c**) mean trophic level ($y = 1.536 - 0.0054x$, $F_{1,12} = 16.10$, $p < 0.001$, $r^2 = 0.54$)

244 and (**d**) directed connectance ($y = 0.220 - 0.0023x$, $F_{1,12} = 18.93$, $p < 0.001$, $r^2 = 0.58$) as

245 stream temperature increased (see Methods for definitions of these food web properties).
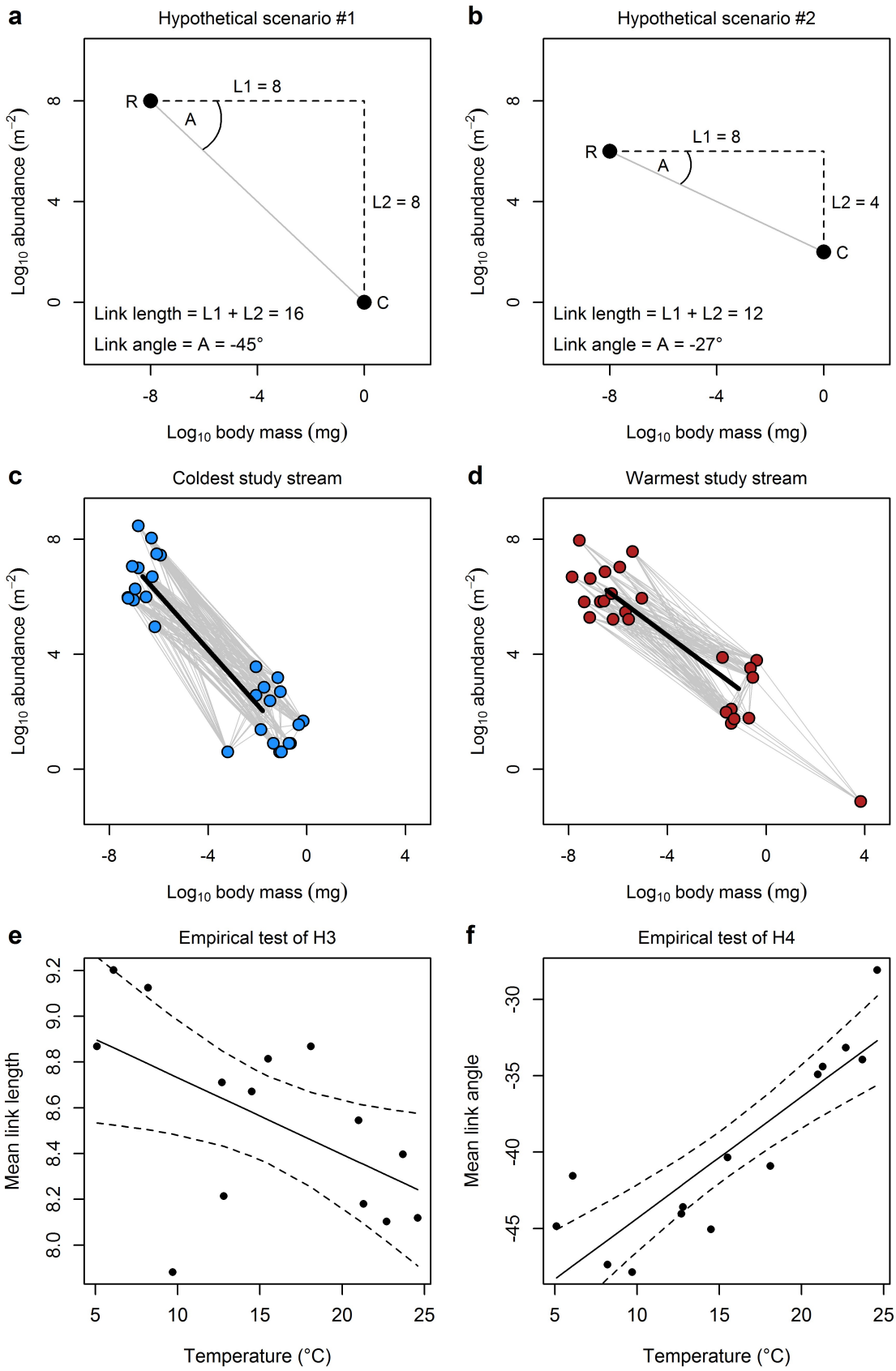

246 **Fig. 2. Temperature effects on energy flux. a**, The length of a trophic link (grey line) is

247 defined as the sum of the number of orders of magnitude of difference in body mass (L1) and

248 abundance (L2) between a consumer (C) and a resource (R)[25]. The angle (A) of a trophic link

249 measures the rate of change in biomass from a consumer to a resource[25]. Here, consumer

250 biomass (mass $\times$ abundance $= 10^0 \times 10^0 = 1$ mg m^{-2}) equals resource biomass ($10^{-8} \times 10^8 = 1$

251 mg m^{-2}), resulting in a link angle of -45°. **b**, A decline in resource abundance and an increase

252 in consumer abundance (relative to panel **a**) results in a shorter link length and a less negative

253 link angle. Here, consumer biomass ($10^0 \times 10^2 = 100$ mg m^{-2}) is greater than resource

254 biomass ($10^{-8} \times 10^6 = 0.01$ mg m^{-2}), resulting in a link angle of -27°. Trivariate food webs for

255 the (**c**) coldest and (**d**) warmest stream in the system, where circles are species, grey lines are

256 feeding interactions, and the thick black lines represent the mean link length and mean link

257 angle of the food web. There was (**e**) a reduction in mean link length ($y = 9.067 - 0.0335x$,

258 $F_{1,12} = 5.04$, $p < 0.001$, $r^2 = 0.24$) and (**f**) a smaller (*i.e.* less negative) mean link angle ($y =$

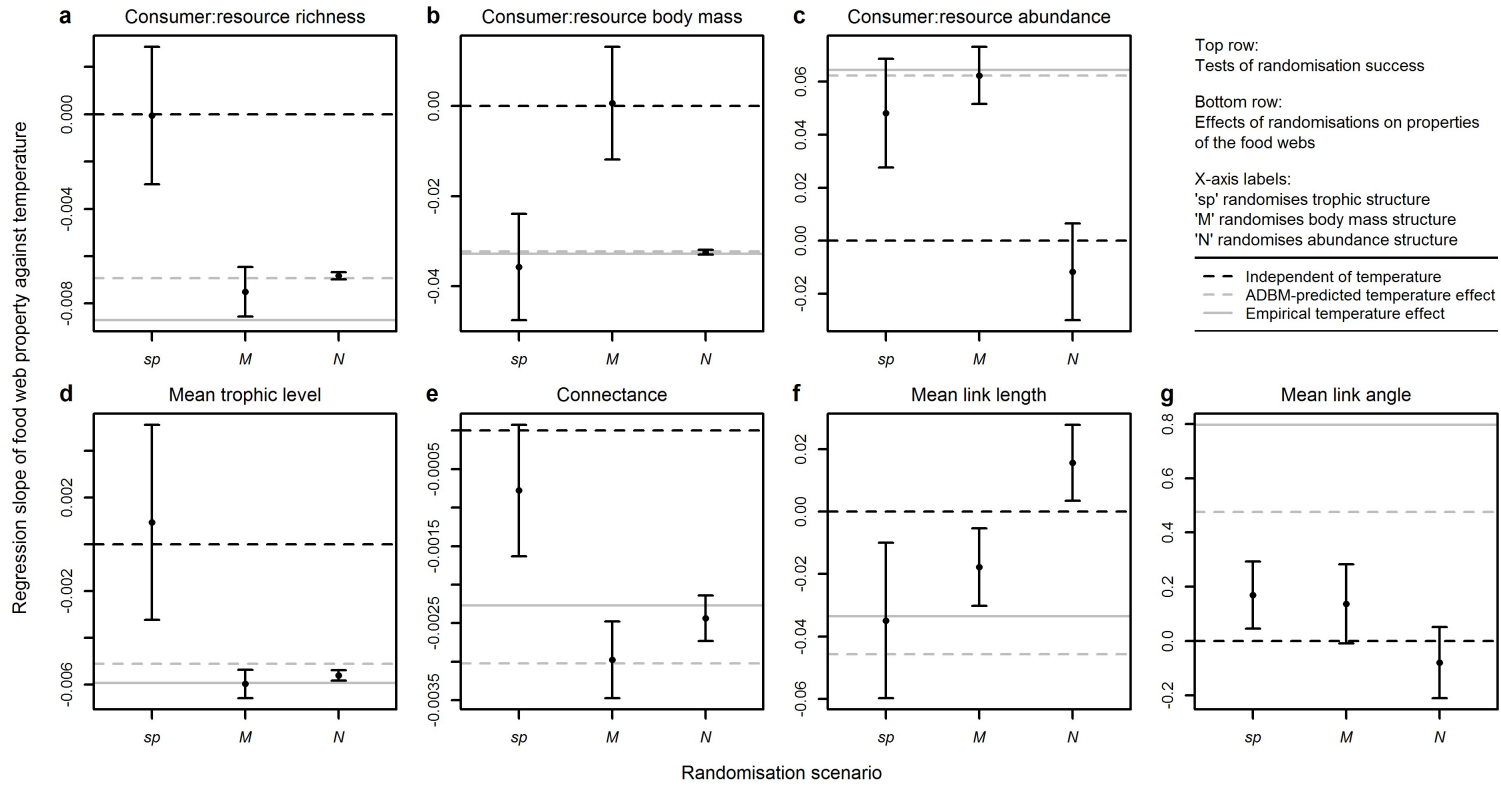259 $-52.30 + 0.797x$, $F_{1,12} = 37.28$, $p < 0.001$, $r^2 = 0.74$) as stream temperature increased.

260 **Fig. 3. Effect of randomisations on temperature dependence of food web properties.** The

261 mean (± standard deviation) of linear regression slopes between food web properties and

262 stream temperature for 1,000 randomisations are shown in the plots. The black dashed line

263 represents a regression slope of zero between a food web property and temperature, *i.e.* the

264 property is independent of temperature. The solid and dashed grey lines represent the

265 empirical and ADBM-predicted regression slope of each food web property against

266 temperature, respectively. **a**, The '*sp*' scenario randomises the species found in a stream and

267 thus the ratio of consumer to resource species richness. **b**, The '*M*' scenario randomises the

268 average body mass of species in the stream and thus the ratio of consumer to resource body

269 mass. **c**, The '*N*' scenario randomises the population abundance of species in the stream and

270 thus the ratio of consumer to resource abundance. The effect of temperature on (**d**) mean

271 trophic level and (**e**) connectance is removed by the '*sp*' scenario. The effect of temperature

272 on (**f**) mean link length and (**g**) mean link angle is removed by the '*N*' scenario. In all other

273 cases, even if the randomisation scenario disrupts the empirical and ADBM-predicted

274 patterns, it maintains the directionality of the temperature effect on the food web property.

275 **Fig. 4. Key determinants of food web properties.** Effect of the ratio of consumer to

276 resource species richness (independent of temperature) on (**a**) mean trophic level ($y = 0.847 +$

277 $1.4044x$, $r^2 = 0.94$) and (**b**) connectance ($y = 0.227 + 0.1952x$, $r^2 = 0.35$) in 1,000 food webs

278 simulated for each of the 14 streams under the '*sp*' scenario (*cf.* Fig. 3). Effect of the log ratio

279 of consumer to resource abundance (independent of temperature) on (**c**) mean link length ($y =$

280 $6.284 - 0.5105x$, $r^2 = 0.32$) and (**d**) mean link angle ($y = -20.37 + 3.297x$, $r^2 = 0.13$) in 1,000

281 food webs simulated for each of the 14 streams under the '*N*' randomisation scenario (*cf.* Fig.

282 3). Parameter estimates are the mean intercept, slope, and r^2 values from 1,000 linear

283 regressions of the relationship across streams (*i.e.* one regression for each randomisation).

284

Fig. 1

a   Coldest study stream

b   Warmest study stream

c   Empirical test of H1

d   Empirical test of H2

Fig. 2

Fig. 3

a Consumer:resource richness
b Consumer:resource body mass
c Consumer:resource abundance
d Mean trophic level
e Connectance
f Mean link length
g Mean link angle

Regression slope of food web property against temperature

Randomisation scenario

Top row:
Tests of randomisation success

Bottom row:
Effects of randomisations on properties
of the food webs

X-axis labels:
'sp' randomises trophic structure
'M' randomises body mass structure
'N' randomises abundance structure

– – – Independent of temperature
– – – ADBM-predicted temperature effect
——— Empirical temperature effect

Fig. 4
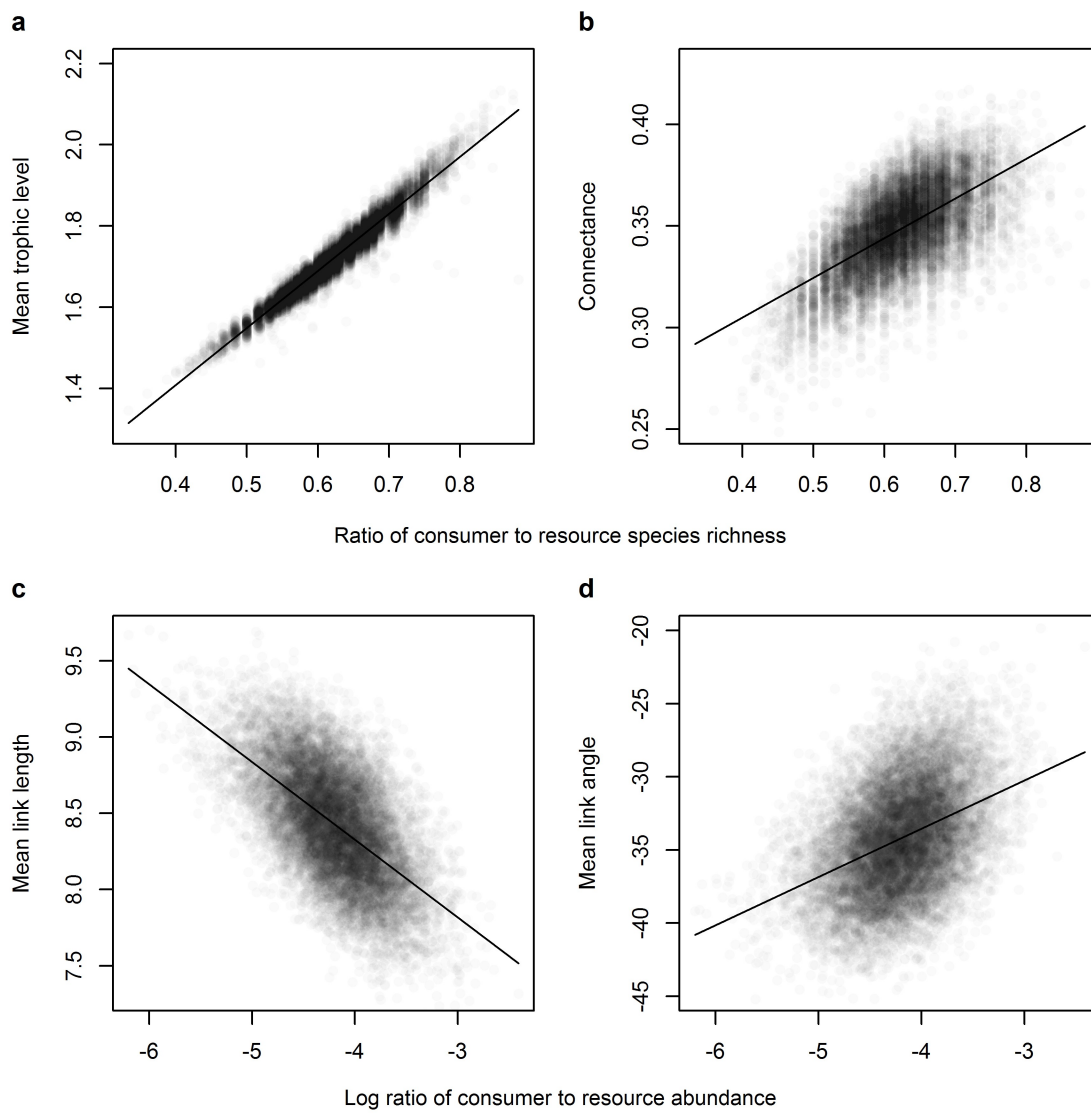
Methods

Stream sampling

Streams were sampled in August 2008 and April 2009 to quantify the three major trophic groups in the system: benthic diatoms (three stone scrapes per stream), macroinvertebrates (five Surber samples per stream), and fish (three-run depletion electrofishing). Yield-effort curves were constructed to verify the efficiency of sampling[13]. We focus on the August 2008 data throughout because they represent the height of the growing season, whereas the April 2009 data are from a time of the year when the streams are in transition. Thus, we only use the latter to determine how consistent the observed patterns are through time. Diatoms and macroinvertebrates were identified to species level under the microscope and counted to estimate population abundance, which was scaled to number of individuals per m^2 based on sampling areas. Average body mass (in milligrams of dry weight) was estimated from linear measurements for at least ten individuals of every species and published length-weight relationships (Tables S4 and S5). Note that diatoms could only be reliably identified to genus level in gut contents, so we calculated the total abundance and abundance-weighted mean body mass of each diatom genus from the species-level data. Nevertheless, we refer to all taxa as species throughout this paper. Body mass measurements of the only fish in the system (brown trout, *Salmo trutta*), were taken on a portable mass balance and converted to dry weight according to a wet weight to dry weight relationship[12]. Precise details of the study system and stream sampling are given in Supplementary Methods.

Overview of food webs

Direct observations of feeding links in nature are preferable to inferences based on indirect evidence, experiments, or prior publications from other study sites[25]. Nevertheless, food web studies are plagued by under-sampling of rare species and links when food webs

318   are constructed entirely based on direct observation and by over-estimation of links when

319   they are entirely inferred from the literature[28,35]. A yield-effort curve for links as a function of

320   cumulative sampling effort should be reported for all direct observations[35], but this is still

321   rarely the case in most food web studies[28]. Here, we performed extensive gut content analysis

322   on organisms collected from our study system and used yield-effort curves to assess the

323   completeness of our sampling effort. We supplemented the under-sampled component with

324   inferences from the literature to achieve the optimum balance between under- and over-

325   estimation of true food web structure.

326   *Gut content analysis*

327   We documented 49,324 feeding interactions from 1,128 individual consumers collected

328   from the Hengill streams using gut content analysis. We employed three different

329   approaches: stomach flushing of fish (5,856 interactions from 109 individuals), acid digestion

330   of macroinvertebrates (25,105 interactions from 289 individuals), and dissection of gut

331   contents (18,363 interactions from 730 individuals). Organisms flushed from fish stomachs

332   were immediately stored in 70% ethanol and later identified under the microscope[13,14].

333   Immersion of macroinvertebrates in 62% nitric acid at 65 °C for 18 hours removes all organic

334   matter except for silicate diatom frustules, enabling accurate identification of diatoms[36], the

335   major primary producers in the streams[13]. A 1 ml sub-sample of the resulting suspension of

336   diatom frustules was pipetted onto a glass coverslip and allowed to dry before fixing to glass

337   slides by adding a drop of naphrax on a 60 °C hotplate. We identified the first 100 diatoms

338   (where possible) encountered in a continuous, non-overlapping 100 µm-wide transect

339   following a fixed route across the slide, which was found to be sufficient for accurately

340   characterising the species present on each slide[36]. Dissection of gut contents allowed us to

341   quantify predation on other macroinvertebrates and feeding interactions with basal resources

342   other than diatoms, *i.e.* coarse particulate organic matter (CPOM, which is > 1 mm), fine

343   particulate organic matter (FPOM, which is < 1 mm), macrophytes, filamentous green algae,

344   microscopic green algae, cyanobacteria, and terrestrial subsidies. Invertebrates were dissected

345   at $20\times$ magnification and the gut contents were mounted onto glass slides with Hoyer's

346   medium. Gut contents were quantified in three randomly chosen fields of view at $200\times$

347   magnification on a compound microscope.

348   *Yield-effort curves*

349   We constructed yield-effort curves using the '*fitspecaccum*' function in the '*vegan*'

350   package in R 3.5.0, where our community dataset was a matrix with rows as unique consumer

351   guts analysed, columns as resource taxa, and values as the number of times each resource

352   taxon was observed in a consumer's gut. We used '*method = "exact"*' and set '*fit*' equal to each

353   of the following models: '*arrhenius*', '*gleason*', '*gitay*', '*lomolino*', '*asymp*', '*gompertz*',

354   '*michaelis-menten*', '*logis*', and '*weibull*'. We chose the best fitting model according to AIC

355   and used the '*predict*' function in the '*stats*' package in R to estimate the predicted number of

356   resource taxa for each consumer, where '*newdata*' was the bigger value from twice the

357   number of guts analysed for that consumer and 50. We carried out this procedure for four

358   different groupings of consumer diet: (1) every consumer species in each stream; (2) every

359   consumer family in each stream; (3) every consumer species in the Hengill region; and (4)

360   every consumer family in the Hengill region.

361   *Food web construction*

362   To construct a food web for a given stream, we started by taking the species list from

363   sampling of that stream in August 2008. We then added links for each species from gut

364   content analysis of those species in that stream. If yield-effort curves suggested that <95% of

365   the diet was described for any species (Fig. S9), we added links for consumers in the same

366   taxonomic family from gut content analysis of those families in that stream. If yield-effort

367   curves suggested that <95% of the diet was described for any family (Fig. S10), we added

368   links for each species from gut content analysis of those species across all streams in the

369   Hengill region. If yield-effort curves suggested that <95% of the diet was described for any

370   species in the Hengill region (Fig. S11), we added links for consumers in the same taxonomic

371   family from gut content analysis of those families across all streams in the Hengill region. If

372   yield-effort curves suggested that <95% of the diet was described for any family in the

373   Hengill region (Fig. S12), we added links described for that species from the literature (Table

374   S6). Just 12.6% of links were added from the literature, with 43.5% of links directly observed

375   from the target stream, and the remaining 43.9% of links directly observed from the Hengill

376   region. From our directly observed links, 74.3% were specific to each consumer species, with

377   just 25.7% inferred from the family level. This constitutes one of the most comprehensive

378   food web datasets ever constructed.

379   *Food web properties*

380   Food webs were visualised and properties were calculated using the '*cheddar*' package

381   in R. The triangular food webs in Fig. 1a,b and the trivariate food webs in Fig. 2c,d were

382   visualised using the '*PlotWebByLevel*' and '*PlotMvN*' functions, respectively. Mean trophic

383   level was calculated using the '*ShortWeightedTrophicLevel*' function, which is the average of

384   the shortest trophic level of a consumer and 1 + the mean trophic level of all its trophic

385   resources. This metric has been shown to closely approximate flow-based trophic level,

386   where each link is weighted according to its relative energetic contribution to the consumer's

387   diet[37]. Connectance was calculated using the '*DirectedConnectance*' function, which is the

388   proportion of possible links in a food web that are realised[38]. Mean link length and mean link

389 angle were calculated from the '*length*' and '*angle*' columns under the '*links*' data frame

390 returned by the '*NvMTriTrophicStatistics*' function. Link lengths describe the distance in

391 mass-abundance space between every consumer and each of its resources in the food web,

392 while link angles describe the biomass of every consumer relative to each of its resources

393 (see Fig. 2a). These metrics are increasingly used to quantify the flux and distribution of

394 biomass through the food web[25,39-42] and provide more precise information than biomass

395 pyramids, which only describe the total biomass at each discrete trophic level (see Fig. S6).

396 The ratio of consumer to resource species richness was calculated as the number of consumer

397 species divided by the number of resource species. The difference in the $\log_{10}$ abundance-

398 weighted arithmetic mean body mass of consumers and of resources was taken as the log

399 ratio of consumer to resource body mass. The difference in the $\log_{10}$ mean abundance of

400 consumers and of resources was taken as the log ratio of consumer to resource abundance.

401 The difference in the $\log_{10}$ mean abundance $\times$ body mass of consumers and of resources was

402 taken as the log ratio of consumer to resource biomass. Temperature effects on food web

403 properties were analysed with linear regressions using the '*lm*' function in the '*stats*' package

404 in R, with each food web property taken in turn as the dependent variable and stream

405 temperature as the explanatory variable.

406 *Allometric diet breadth model*

407   The allometric diet breadth model (ADBM) is a model of food web structure based on

408 optimal foraging theory. It predicts the qualitative structure of real food webs, often to a high

409 degree of accuracy[16]. By incorporating the temperature dependence of foraging traits, the

410 model has also been shown as a useful framework for predicting the effects of temperature on

411 food web connectance[10]. The ADBM predicts the diet k of each consumer j that maximises

412 the rate of energy intake:

22

$$413 \quad \frac{\sum_{i=1}^{k} N_i a_{ij} E_i}{1 + \sum_{i=1}^{k} N_i a_{ij} h_{ij}}, \qquad (1)$$

414   where N_i is the density of resource species i, a_{ij} is the attack rate of consumer species j on

415   species i, ε_i is the net energy gained by consumption of an individual of species i, and h_{ij} is

416   the time taken for species j to handle an individual of species i.

417   The body mass and temperature dependence of a_{ij} can be described as:

$$418 \quad a_0 M_i^{a_i} M_j^{a_j} e^{E_a \frac{T-T_0}{kTT_0}}, \qquad (2)$$

419   where a_0 is a normalisation constant for attack rate, M_i is resource body mass (in mg), M_j is

420   consumer body mass (in mg), a_i and a_j are allometric exponents, E_a is the activation energy of

421   attack rate (in eV), T is environmental temperature (in K), T_0 sets the intercept of the

422   temperature relationship at T_0 rather than at zero Kelvin, and k is the Boltzmann constant

423   (8.618×10^{-5} eV K^{-1}). The value of E_i is determined by the proportion of dry-to-wet mass in

424   each organism[43,44], ε_i, and may vary with temperature[45], but for simplicity, we assumed here

425   that it would be directly proportional to body mass in all streams[10,16], *i.e.* $E_i = \varepsilon_i M_i$. See Table

426   S7 for a list of all parameter values used in the current study and Figs. S13-S16 for an

427   exploration of the sensitivity of key food web properties to the chosen parameter values.

428   The body mass and temperature dependence of h_{ij} can be described as:

$$429 \quad \frac{h_0}{h_b - \dfrac{M_i}{M_j}} e^{E_h \frac{T-T_0}{kTT_0}}, \qquad (3)$$

430   where h_0 is a normalisation constant for handling time, h_b is a critical mass ratio, and E_h is the

431   activation energy of handling time (in eV). Note that $h_{ij} = \infty$ if $M_i \, / \, M_j \geq h_b$. We let $h_b =$

432      $b_0 M_j^{\,b}$, where $b_0 = 1$ with dimensions that cancel those of M^b, because resource body mass

433   has been shown to vary with consumer body mass according to a power-law[46]. Note that we

434   used a ratio handling time function in Equation 3, rather than a power handling time function

435   because the latter is generally shown to have weaker predictive power[16] and was found to be

436   a poor predictor of empirical food web structure in the Hengill streams. The values for each

437   parameter that were used in the current study are listed in Table S7.

438   It is important to note that the estimates of food web structure based on the ADBM are

439   independent of the empirical quantification of food web structure using dietary analysis. The

440   former relies solely on the body mass and abundance information for each species to

441   determine food web links, whereas the latter determines the links from direct observation in

442   gut contents (>87% of cases) or inference from the literature. Thus, empirical measurements

443   of mean trophic level and connectance are completely independent of the ADBM predictions

444   of these metrics. While mean link length and mean link angle incorporate body mass and

445   abundance information, their values are determined by how consumers and their resources

446   are distributed in mass-abundance space, *i.e.* there is a major contribution of independent

447   trophic link data to these metrics.

448   *Randomisation scenarios*

449   We used the ADBM framework to simulate 1,000 food webs for each of our 14 study

450   streams according to three different randomisation scenarios. In the '*sp*' scenario, we

451   randomly selected *n* species from the regional species pool (where *n* is the number of species

452   in a given stream), with the actual body mass and abundance for each species per stream, or

453   the body mass and abundance from the stream of closest temperature when a species was not

454   found in a stream. This scenario destroyed the ratio of consumer to resource species richness

455   by changing the number of species belonging to each major trophic group (*i.e.* diatoms,

456   macroinvertebrates, or fish) in each stream, but approximately maintained the ratios of

457 consumer to resource body mass and abundance within each stream (Fig. 3a-c). In the 'M'

458 scenario, we maintained the species found in a stream and their population abundances in that

459 stream, but randomly chose body masses from the same major trophic groups in the regional

460 species pool. This scenario destroyed the ratio of consumer to resource body mass, but

461 approximately maintained the ratios of consumer to resource species richness and abundance

462 within each stream (Fig. 3a-c). In the 'N' scenario, we maintained the species found in a

463 stream and their mean body masses in that stream, but randomly chose abundances from the

464 same major trophic groups in the regional species pool. This scenario destroyed the ratio of

465 consumer to resource abundance, but approximately maintained the ratios of consumer to

466 resource species richness and body mass within each stream (Fig. 3a-c).

467 **Data and Code Availability:**

468   The data and R code that support the findings of this study are available from the first

469 author upon reasonable request.

470 **Additional References:**

471 35   Cohen, J. E. *et al.* Improving food webs. *Ecology* **74**, 252-258 (1993).

472 36   Gordon, T. A. C., Neto-Cerejeira, J., Furey, P. C. & O'Gorman, E. J. Changes in

473   feeding selectivity of freshwater invertebrates across a natural thermal gradient.

474   *Current Zoology* **64**, 231-242 (2018).

475 37   Williams, R. J. & Martinez, N. D. Limits to trophic levels and omnivory in complex

476   food webs: Theory and data. *American Naturalist* **163**, 458-468 (2004).

477 38   Martinez, N. D. Artifacts or attributes - effects of resolution on the little-rock lake

478   food web. *Ecological Monographs* **61**, 367-392 (1991).

479 39   Clitherow, L. R., Carrivick, J. L. & Brown, L. E. Food web structure in a harsh

480   glacier-fed river. *PloS One* **8**, e60899 (2013).

481   40   Perkins, D. M. *et al.* Bending the rules: exploitation of allochthonous resources by a

482   top-predator modifies size-abundance scaling in stream food webs. *Ecology letters* **21**,

483   1771-1780 (2018).

484   41   Thompson, M. S. *et al.* Large woody debris "rewilding" rapidly restores biodiversity

485   in riverine food webs. *Journal of applied ecology* **55**, 895-904 (2018).

486   42   Woodward, G. *et al.* Climate change impacts in multispecies systems: drought alters

487   food web size structure in a field experiment. *Philosophical Transactions of the Royal*

488   *Society B: Biological Sciences* **367**, 2990-2997 (2012).

489   43   James, D. A. *et al.* A generalized model for estimating the energy density of

490   invertebrates. *Freshwater Science* **31**, 69-77 (2011).

491   44   Hartman, K. J. & Brandt, S. B. Estimating energy density of fish. *Transactions of the*

492   *American Fisheries Society* **124**, 347-355 (1995).

493   45   Converti, A., Casazza, A. A., Ortiz, E. Y., Perego, P. & Del Borghi, M. Effect of

494   temperature and nitrogen concentration on the growth and lipid content of

495   *Nannochloropsis oculata* and *Chlorella vulgaris* for biodiesel production. *Chemical*

496   *Engineering and Processing: Process Intensification* **48**, 1146-1151 (2009).

497   46   Riede, J. O. *et al.* Stepping in Elton's footprints: a general scaling model for body

498   masses and trophic levels across ecosystems. *Ecology Letters* **14**, 169-178 (2011).